ChemComm

COMMUNICATION

View Article Online
View Journal | View Issue

Cite this: *Chem. Commun.*, 2018, **54**, 13427

Received 25th October 2018,
Accepted 6th November 2018

DOI: 10.1039/c8cc08530g

rsc.li/chemcomm

Cell membrane camouflaged magnetic nanoparticles as a biomimetic drug discovery platform†

Yusi Bu,[ab] Qi Hu,[ab] Ruifang Ke,[ab] Yue Sui,[ab] Xiaoyu Xie *[ab] and Sicen Wang*[ab]

We report a novel biomimetic drug discovery platform using high expression epidermal growth factor receptor (EGFR) HEK 293 cell membrane camouflaged magnetic nanoparticles. The EGFR/magnetic cell membrane nanoparticles (MCMNs) integrated desirable magnetic features and special binding bioaffinity. Application of this drug-targeting concept is expected to pave ways to a new drug discovery strategy.

As a rich source of compounds for new drug discovery, natural products have made dramatic contribution to cancer chemotherapy.[1] Many bioactive compounds screened from natural products like taxol[2] and camptothecin[3] show remarkable efficacy against refractory cancers. The traditional method for screening and discovering bioactive compounds is to isolate a single compound first from complex plant extracts and then determine its bioactivity *via* classic pharmacological methods.[4] However, this complicated process is proved to be time-consuming and arduous restricting the application of natural products for drug discovery. Hence, an efficient and timesaving method is in urgent need. Magnetic nanotechnology has attracted worldwide attention because of its unique properties such as special magnetic features and high surface area. As demonstrated by M. Yasuda, magnetic beads immobilized with SIRT6 protein were achieved to screen novel inhibitors from plant extracts.[5] Different molecules like proteins,[6] peptides,[7] enzymes[8] and other micromolecules[9] were successfully functionalized onto nanoparticles and provided nanomaterials with different distinct properties. However, these functionalization approaches still remain inadequate in simulating the complex interfaces *in vivo*. Moreover, the fixation can potentially change the native structure of proteins that are stabilized in lipid bilayers *in vivo*, leading to possible false positives or false negatives of the screening.[10] Thus, the development of functionalization to nanomaterials that is able to specifically target bioactive compounds is highly desirable.

Cell membranes are major biological interfaces keeping living systems and the external environment apart, and membrane proteins are major targets for drug screening. It has been estimated that over 50% pharmaceuticals interact with specific cell membrane receptors.[11] To screen drugs against membrane receptors, the cell membrane cloaked nanoparticle strategy is getting increasing attention because of the ability of the cell membrane to replicate the integral surface properties. The biomimetic nanoparticles showed numerous desirable characteristics such as specific targeting ability,[12] retention of natural structures of membrane proteins[13] and right-side-out membrane coverage.[14] The proposed technology has been applied for targeting cancer cells,[15] toxins,[12,16] viruses[17] and immunoglobulin.[18] As demonstrated by Hu *et al.*, platelet membrane coated polymeric nanoparticles with bacteria-targeting capability were successfully prepared and docetaxel and vancomycin were targetedly delivered.[10] In addition, Hu also reported that functionalization with a red cell membrane enabled biomimetic nanosponge targeting of pore-forming toxins.[12] These studies demonstrate that cell membrane cloaked nanoparticles have exhibited great potential as an intriguing tool for drug discovery.

The epidermal growth factor receptor (EGFR) is a widely distributed cell membrane receptor which has been proved to have a close association with malignant tumors such as lung cancer and breast cancer.[19] Therefore, a high expression EGFR cell membrane could be an effective tool for screening potential EGFR antagonists. In this study, magnetic nanoparticles were cloaked by high expression EGFR HEK 293 cell membrane targeting potential anti-tumor compounds from traditional Chinese medicines (TCMs), which demonstrated desirable magnetic features and special binding bioaffinity. Thus, our study may open a novel avenue for rapid targeting and screening of bioactive compounds in drug discovery.

The EGFR/MCMN preparation process is illustrated in Fig. 1. Fe_3O_4 particles were synthesized as a magnetic core to guarantee

[a] *School of Pharmacy, Health Science Center, Xi'an Jiaotong University, Xi'an 710061, China. E-mail: xiexiaoyu@xjtu.edu.cn, wangsc@mail.xjtu.edu.cn*
[b] *Shaanxi Engineering Research Center of Cardiovascular Drugs Screening & Analysis, Xi'an 710061, China*

† Electronic supplementary information (ESI) available. See DOI: 10.1039/c8cc08530g

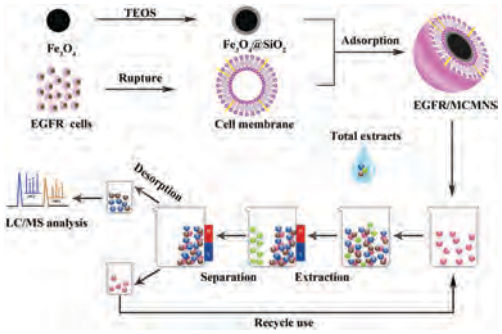

Fig. 1 Schematic illustration of high expression EGFR HEK 293 cell membrane coated magnetic nanoparticles for bioactive compound extraction.

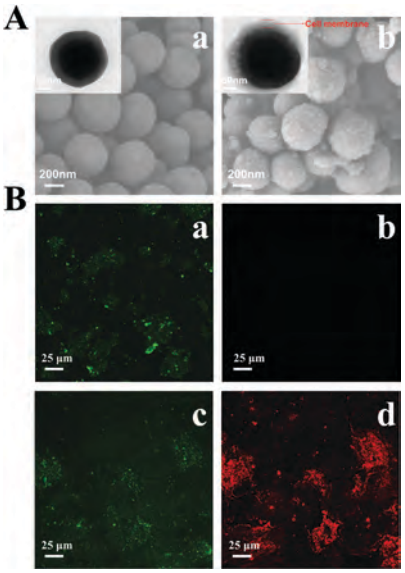

Fig. 2 (A) TEM and SEM images of (a) MNMNs and (b) EGFR/MCMNs; (B) confocal microscopy images of (a and b) MNMNs and (c and d) EGFR/MCMNs: (a and c) green fluorescence images and (b and d) red fluorescence images.

that the final materials were magnetic-responsive. After coating with a SiO_2 shell, Fe_3O_4 nanoparticle surfaces were full of polar silanol groups (Si–OH), which enabled the cell membrane to be easily adsorbed. An optimized amount of the cell membrane with the special self-fusion characteristics could fully cloak the Fe_3O_4@SiO_2. To obtain more effective EGFR/MCMNs, the approach to disrupt cells, the ratio of Fe_3O_4@SiO_2 to cell membrane quantity and the adsorption time were further optimized (ESI†) as shown in Tables S1 and S2 (ESI†).

Firstly, the morphological characteristics of the resultant nanoparticles were investigated by transmission electron microscopy (TEM) and scanning electron microscopy (SEM). It can be observed that after tetraethoxysilane modification and cell membrane coating, Fe_3O_4@SiO_2, magnetic non-cell membrane nanoparticles (MNMNs) and EGFR/MCMNs still revealed the fine spherical shape (Fig. S1B, ESI,† and Fig. 2Aa and b). The mean diameter of the Fe_3O_4@SiO_2 increased to around 380–440 nm (Fig. S1B and D, ESI†). As presented in Fig. 2Ab, after coating on the cell membrane, the EGFR/MCMNs showed consistent unilamellar membrane coarse coating approximately 15 nm thicker than that of MNMNs. Moreover, to validate the successful functionalization with the adhesion molecules of high expression EGFR HEK 293 cells, the presence of membrane protein and phospholipid on the surface of EGFR/MCMNs was determined morphologically by confocal microscopy. Fe_3O_4@SiO_2 nanoparticles were labelled with fluorescein isothiocyanate (FITC, green fluorescence) and the cell membrane lipid bilayer was labelled with 1,1′-dioctadecyl-3,3,3′,3′-tetramethylindocarbocyanine perchlorate (DiI, a cell membrane lipid bilayer red fluorescence label). As shown in Fig. 2B, green fluorescence was observed verifying the existence of nanoparticles on EGFR/MCMNs and MNMNs. And significant red fluorescence is observed in Fig. 2Bd, indicating the coating of the membrane lipid bilayer on the surface of nanoparticles. By contrast, red fluorescence is hardly observed in Fig. 2Bb showing the absence of cell membranes on MNMNs. Overall, these results demonstrated a successful location of cell membranes onto nanoparticles. Moreover, EGFR/MCMNs showed satisfactory superparamagnetic properties with saturation magnetization of 15.28 emu g^{-1} (Fig. S2A, ESI†).

Fourier transform infrared spectroscopy (Fig. S2B, ESI†) investigation validated that Fe_3O_4 was successfully prepared with a SiO_2 layer providing abundant Si–OH to adsorb cell membranes. Chemical composition investigation (Fig. S2C, ESI†) showed the presence of the N 1s peak at 400.1 eV that was donated by proteins on the cell membrane, indicating that the cell membrane was successfully grafted onto the surface of Fe_3O_4@SiO_2. Lastly, X-ray diffraction patterns suggested that the preparation process of EGFR/MCMNs had no influence on its magnetite core (Fig. S2D, ESI†).

Secondly, the adsorption capacity was evaluated by static adsorption experiments. Gefitinib was selected as a positive medicine to EGFR.[19] As shown in Fig. 3A, the binding amounts for gefitinib on EGFR/MCMNs increased quickly at first in the range 20–3000 mg L^{-1} and then slowed down and achieved a saturated plateau with a binding capacity of 200 mg g^{-1}. Moreover, the binding amounts on MNMNs and HEK 293/MCMNs showed a similar trend to EGFR/MCMNs but with a poor binding capacity. It can be concluded that EGFR/MCMNs have higher selective adsorption ability than gefitinib. The obtained data of the static adsorption experiment were analyzed *via* Freundlich, Langmuir, Scatchard and Dubinin–Radushkevich isotherms,[20] respectively (Fig. 3B and Table S3, ESI†). It was obvious that the Freundlich isotherm (FI, ESI†) could accurately model EGFR/MCMNs, MNMNs and HEK 293/MCMNs in the measured concentration with the highest correlation coefficient (r, 0.9916 for EGFR/MCMNs, 0.9062 for MNMNs and 0.9773 for HEK 293/MCMNs). After calculated by the corresponding affinity distribution (AD, Fig. S3, ESI†),[20,21] the distribution of binding sites exponentially decayed in all three materials. Moreover, the number of binding sites for EGFR/MCMNs was much higher than that of MNMNs in a given affinity energy. All binding parameters are shown in Table S4 (ESI†). Within a given concentration window, the values of apparent number of binding sites for EGFR/MCMNs are 13 times greater than those of MNMNs

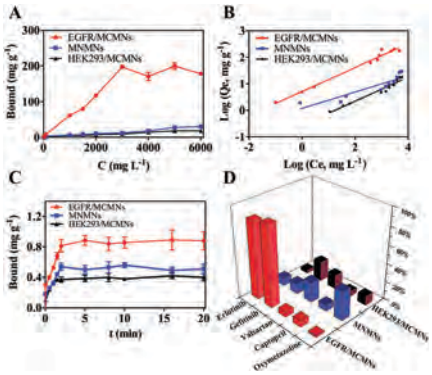

Fig. 3 (A) Static adsorption isotherm curves; (B) FI analysis of gefitinib on EGFR/MCMNs, MNMNs and HEK 293/MCMNs; (C) adsorption kinetics of gefitinib on EGFR/MCMNs, MNMNs and HEK 293/MCMNs; (D) elution recoveries of five compounds on EGFR/MCMNs, MNMNs and HEK 293/MCMNs.

and 18 times greater than those of HEK 293/MCMNs. Thus, it could be concluded that the coating of EGFR of the cell membrane played an important role in heterogeneity of the EGFR/MCMNs.

The adsorption kinetics is an important factor in practical applications, which is shown in Fig. 3C. The adsorption amount of gefitinib on EGFR/MCMNs increased quickly in the first 2 minutes and reached equilibrium after 10 minutes due to saturation of adsorption capacity. The adsorption behavior of gefitinib on MNMNs and HEK 293/MCMNs showed a similar trend, while the adsorption capacity was much lower than that on EGFR/MCMNs. The results showed that the mass transfer rate of gefitinib on EGFR/MCMN sorbents was very fast, which was beneficial to quickly screen bioactive compounds in practical applications. In order to estimate the mass transfer mechanism, the pseudo-first-order (ESI†) and pseudo-second-order equations (ESI†) were fitted in the kinetic data.[22] The results showed that r values of the pseudo-first adsorption model for EGFR/MCMNs and MNMNs were both higher than those of the pseudo-second adsorption model (Table S5, ESI†). In the pseudo-first-order model, the occupation of adsorption sites' rate is proportional to the number of unoccupied sites.[23] Thus, the kinetic adsorption for gefitinib on EGFR/MCMNs can be described by the pseudo-first-order model very well. In addition, four different kinds of medicines acting on different receptors were selected to be pretreated by EGFR/MCMNs to investigate the selectivity of EGFR/MCMNs for active compounds. Erlotinib[19] and gefitinib blocking the EGFR tyrosine kinase protein were chosen as the positive control. Valsartan, captopril and oxymetazoline were selected as the negative control and extracted *via* the same procedure. As displayed in Fig. 3D, erlotinib and gefitinib were well screened by EGFR/MCMNs with high recoveries while negligible recoveries were detected on MNMNs. As for valsartan, captopril and oxymetazoline, low recoveries were observed on both EGFR/MCMNs and MNMNs. The successful coating of the cell membrane contributes to the good selectivity of EGFR/MCMNs.

Thirdly, optimization for EGFR/MCMNs in the extraction procedure was conducted. As can be seen in Fig. S4Aa (ESI†), isopropyl alcohol–50 mmol L^{-1} Na_2HPO_4 (15 : 85, v/v) gave a good washing performance with stable selectivity on the desorption of positive medicine from the MNMNs. Moreover, DMSO exhibited the highest desorption capability towards gefitinib on EGFR/MCMNs. The poor desorption capability of the five eluents for gefitinib on HEK 293/MCMNs might due to the great loss of gefitinib during the loading procedure at the beginning. The bound amount of gefitinib increased with increasing adsorbent amount from 1 to 15 mg and became stable when the adsorbent amounts were greater than 15 mg (Fig. S4B, ESI†). In addition, 50 mg EGFR/MCMNs were selected as the adsorbent amount and 20 min elution time and 5 mL elution volume (ESI†) can achieve satisfactory extraction efficiency (Fig. S4C and D, ESI†). Due to the binding sites of gefitinib, EGFR/MCMNs provide a new opportunity to screen bioactive compounds which are actually binding with the intracellular domain of EGFR. This bionic conception broadens its approach to screen bioactive compounds and tends to be effective.

Lastly, the prepared EGFR/MCMNs were applied as the solid phase extraction sorbents to selectively extract potential bioactive compounds from *Radix Aconiti* (RA). 50 mg EGFR/MCMNs were added to the sample solution. Then the suspension was shaken for 20 min at 37 °C. The analytes were washed from the EGFR/MCMNs with 5 mL isopropyl alcohol–50 mmol L^{-1} Na_2HPO_4 (15 : 85, v/v) before using 5 mL DMSO eluent by sonication for 10 min. Then the initial extract solution of RA, the solution after loading, the solution after washing and the eluent were analysed and their chromatograms are shown in Fig. 4. It can be seen that many compounds were barely retained in EGFR/MCMNs during the loading process (Fig. 4b) and a few bound compounds were washed off after the rinsing procedure (Fig. 4c) compared with the initial RA extracts (Fig. 4b). Two main peaks are observed in Fig. 4d in the analysis of the eluent solution extracted by EGFR/MCMNs, which could be inferred as bioactive constituents. The two screened compounds were further analyzed using the TOFMS system. As shown in Fig. 4, peaks 1 and 2 were identified respectively as benzoylmesaconine and hypaconitine. Standard benzoylmesaconine and hypaconitine's chromatogram and mass spectrum further confirmed the conclusion. The pharmacological effects (ESI†) and interaction simulations (ESI†) showed the good inhibition of the two tested compounds as well as their underlying mechanisms and binding models. The results indicated that the proposed novel affinity magnetic sample pretreatment technique was a reliable and efficient method (Fig. S5, ESI†).

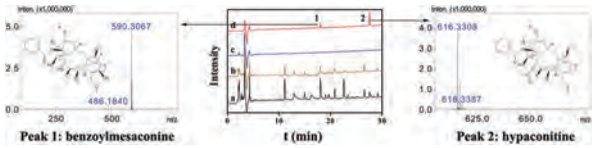

Fig. 4 Chromatograms of the extracts from RA using EGFR/MCMNs. (a) Initial solution, (b) solution after loading, (c) solution after washing, (d) solution after eluting and TOFMS and chemical construction results of peaks 1 and 2 in eluent solution.

In summary, through camouflaged magnetic nanoparticles with a high expression EGFR HEK 293 cell membrane, the EGFR/MCMNs were prepared with desirable magnetic features and special binding bioaffinity. Moreover, two bioactive compounds such as benzoylmesaconine and hypaconitine were screened in real application. The preliminary pharmacological assays showed the potential anti-tumor activities of the screened compounds. This work shows cell membrane coated magnetic nanoparticles' unique function in exploiting bioactive compounds for targeting. The application of this drug-targeting concept represents a promising platform for new drug discovery strategies. In addition, the proposed nanosystem connects artificial nanoparticles with biological entities and highlights inspired new insights and methodologies to develop the integration of cell membranes with nanoparticle platforms.

We gratefully acknowledge the National Natural Science Foundation of China (No. 81503033 and 81673398) and the Natural Science Foundation of Shaanxi province (No. 2016JQ8016) for financial support.

Conflicts of interest

There are no conflicts to declare.

Notes and references

1 (*a*) J. Mann, *Nat. Rev. Cancer*, 2002, **2**, 143–148; (*b*) G. Kallifatidis, J. J. Hoy and B. L. Lokeshwar, *Semin. Cancer Biol.*, 2016, **40–41**, 160–169; (*c*) A. Bishayee and G. Sethi, *Semin. Cancer Biol.*, 2016, **40–41**, 1–3.

2 (*a*) M. C. Wani, H. L. Taylor, M. E. Wall, P. Coggon and A. T. McPhail, *J. Am. Chem. Soc.*, 1971, **93**, 2325–2327; (*b*) S. M. Tolaney, W. T. Barry, C. T. Dang, D. A. Yardley, B. Moy, P. K. Marcom, K. S. Albain, H. S. Rugo, M. Ellis, I. Shapira, A. C. Wolff, L. A. Carey, B. A. Overmoyer, A. H. Partridge, H. Guo, C. A. Hudis, I. E. Krop, H. J. Burstein and E. P. Winer, *N. Engl. J. Med.*, 2015, **372**, 134–141.

3 (*a*) M. E. Wall, M. C. Wani, C. E. Cook, K. H. Palmer, A. A. McPhail and G. A. Sim, *J. Am. Chem. Soc.*, 1966, **88**, 3888–3890; (*b*) K. M. Camacho, S. Kumar, S. Menegatti, D. R. Vogus, A. C. Anselmo and S. Mitragotri, *J. Controlled Release*, 2015, **210**, 198–207.

4 A. L. Harvey, R. Edrada-Ebel and R. J. Quinn, *Nat. Rev. Drug Discovery*, 2015, **14**, 111–129.

5 M. Yasuda, D. R. Wilson, S. D. Fugmann and R. Moaddel, *Anal. Chem.*, 2011, **83**, 7400–7407.

6 S. Y. New, K. M. Aung, G. L. Lim, S. Hong, S. K. Tan, Y. Lu, E. Cheung and X. Su, *Anal. Chem.*, 2014, **86**, 2361–2370.

7 J. Xie, K. Chen, H.-Y. Lee, C. Xu, A. R. Hsu, S. Peng, X. Chen and S. Sun, *J. Am. Chem. Soc.*, 2008, **130**, 7542–7543.

8 Y. Li, J. Xu, Y. Chen, Z. Mei and Y. Xiao, *J. Chromatogr. A*, 2015, **1425**, 8–16.

9 (*a*) Y. N. Tan, X. Su, Y. Zhu and J. Y. Lee, *ACS Nano*, 2010, **4**, 5101–5110; (*b*) H. Groult, N. Poupard, F. Herranz, E. Conforto, N. Bridiau, F. Sannier, S. Bordenave, J. M. Piot, J. Ruiz-Cabello, I. Fruitier-Arnaudin and T. Maugard, *Biomacromolecules*, 2017, **18**, 3156–3167.

10 C.-M. J. Hu, R. H. Fang, K.-C. Wang, B. T. Luk, S. Thamphiwatana, D. Dehaini, P. Nguyen, P. Angsantikul, C. H. Wen, A. V. Kroll, C. Carpenter, M. Ramesh, V. Qu, S. H. Patel, J. Zhu, W. Shi, F. M. Hofman, T. C. Chen, W. Gao, K. Zhang, S. Chien and L. Zhang, *Nature*, 2015, **526**, 118–121.

11 (*a*) D. Jürgen, *Science*, 2000, **287**, 1960–1964; (*b*) S. Majd and M. Mayer, *Angew. Chem., Int. Ed.*, 2005, **44**, 6697–6700.

12 (*a*) C. M. Hu, R. H. Fang, J. Copp, B. T. Luk and L. Zhang, *Nat. Nanotechnol.*, 2013, **8**, 336–340; (*b*) L. Rao, L. L. Bu, J. H. Xu, B. Cai, G. T. Yu, X. Yu, Z. He, Q. Huang, A. Li, S.-S. Guo, W.-F. Zhang, W. Liu, Z. J. Sun, H. Wang, T.-H. Wang and X.-Z. Zhao, *Small*, 2015, **11**, 6225–6236; (*c*) X. Ren, R. Zheng, X. Fang, X. Wang, X. Zhang, W. Yang and X. Sha, *Biomaterials*, 2016, **92**, 13–24.

13 (*a*) C. M. Hu, L. Zhang, S. Aryal, C. Cheung, R. H. Fang and L. Zhang, *Proc. Natl. Acad. Sci. U. S. A.*, 2011, **108**, 10980–10985; (*b*) Q. Fu, P. Lv, Z. Chen, D. Ni, L. Zhang, H. Yue, Z. Yue, W. Wei and G. Ma, *Nanoscale*, 2015, **7**, 4020–4030; (*c*) R. H. Fang, C. M. Hu, B. T. Luk, W. Gao, J. A. Copp, Y. Tai, D. E. O'Connor and L. Zhang, *Nano Lett.*, 2014, **14**, 2181–2188.

14 C. M. Hu, R. H. Fang, B. T. Luk, K. N. Chen, C. Carpenter, W. Gao, K. Zhang and L. Zhang, *Nanoscale*, 2013, **5**, 2664–2668.

15 (*a*) Z. Chen, P. Zhao, Z. Luo, M. Zheng, H. Tian, P. Gong, G. Gao, H. Pan, L. Liu, A. Ma, H. Cui, Y. Ma and L. Cai, *ACS Nano*, 2016, **10**, 10049–10057; (*b*) J. Li, Y. Ai, L. Wang, P. Bu, C. C. Sharkey, Q. Wu, B. Wun, S. Roy, X. Shen and M. R. King, *Biomaterials*, 2016, **76**, 52–65.

16 Z. Pang, C.-M. J. Hu, R. H. Fang, B. T. Luk, W. Gao, F. Wang, E. Chuluun, P. Angsantikul, S. Thamphiwatana, W. Lu, X. Jiang and L. Zhang, *ACS Nano*, 2015, **9**, 6450–6458.

17 H. W. Chen, Z. S. Fang, Y. T. Chen, Y. I. Chen, B. Y. Yao, J. Y. Cheng, C. Y. Chien, Y. C. Chang and C. J. Hu, *ACS Appl. Mater. Interfaces*, 2017, **9**, 39953–39961.

18 (*a*) X. Wei, J. Gao, R. H. Fang, B. T. Luk, A. V. Kroll, D. Dehaini, J. Zhou, H. W. Kim, W. Gao, W. Lu and L. Zhang, *Biomaterials*, 2016, **111**, 116–123; (*b*) J. A. Copp, R. H. Fang, B. T. Luk, C. M. Hu, W. Gao, K. Zhang and L. Zhang, *Proc. Natl. Acad. Sci. U. S. A.*, 2014, **111**, 13481–13486.

19 (*a*) J. Richard, C. Sainsbury, G. Needham, J. Farndon, A. Malcolm and A. Harris, *Lancet*, 1987, **329**, 1398–1402; (*b*) T. J. Lynch, D. W. Bell, R. Sordella, S. Gurubhagavatula, R. A. Okimoto, B. W. Brannigan, P. L. Harris, S. M. Haserlat, J. G. Supko, F. G. Haluska, D. N. Louis, D. C. Christiani, J. Settleman and D. A. Haber, *N. Engl. J. Med.*, 2004, **350**, 2129–2139; (*c*) R. Rosell, *et al.*, *Lancet Respir. Med.*, 2017, **5**, 435–444.

20 (*a*) Y. Bu, X. He, Q. Hu, C. Wang, X. Xie and S. Wang, *Sci. Rep.*, 2017, **7**, 3569; (*b*) A. Kasprzak and M. Poplawska, *Chem. Commun.*, 2018, **54**, 8547–8562; (*c*) Y. Bu, Q. Hu, K. Xu, X. Xie and S. Wang, *J. Mater. Chem. B*, 2018, **6**, 624–633.

21 F. F. Chen, R. Wang and Y. P. Shi, *Talanta*, 2012, **89**, 505–512.

22 H. Minato, M. Murai, T. Watanabe, S. Matsui, M. Takizawa, T. Kureha and D. Suzuki, *Chem. Commun.*, 2018, **54**, 932–935.

23 G. Cheng, Y. Chai, J. Chen, J. Chen, Q. Zhang, S. Ji, L. Ou and Y. Yu, *Chem. Commun.*, 2017, **53**, 7744–7747.

